



Assessing the cold island effect of urban parks in metropolitan cores: a case study of Hangzhou, China

Peng Tian¹ · Jialin Li^{1,2,3} · Ruiliang Pu⁴ · Luodan Cao¹ · Yongchao Liu¹ · Haitao Zhang¹

Received: 12 November 2022 / Accepted: 31 May 2023 / Published online: 13 June 2023
© The Author(s), under exclusive licence to Springer-Verlag GmbH Germany, part of Springer Nature 2023

Abstract

As the oasis area in the city, urban park plays an extremely prominent role in the regulation and improvement of the urban ecological environment, especially the local thermal environment, and has become one of the significant ways to reduce the urban heat island (UHI) effect. Our study comprehensively considers the maximum cooling distance and spatial continuity of urban parks, takes 30 parks in Hangzhou, and analyzed their influencing factors to comprehensively explore the park cooling effect. The results showed that the land cover shifted drastically during 2000–2020, and the built-up land area increased greatly, which aggravated the UHI effect. The high UHI value of Hangzhou was concentrated in the city center and presented a spreading trend from north to south. Different types of urban parks presented different cold island effects, with comprehensive parks and ecological parks having the largest cooling area, and community parks exhibit better accumulative cooling effect. In addition, the park's own characteristics (perimeter, area, shape index) and inner and surrounding landscapes were significantly correlated with the park's cooling effect (park cooling area and park cooling efficiency). Our study comprehensively considered the cooling effect of parks from the maximum and accumulative perspectives and provides theoretical and practical guidance for the construction and planning of urban parks, thereby enhancing the well-being of urban residents.

Keywords LST · Cooling island effect · Urban parks · Park cooling intensity · Hangzhou

Introduction

Global urbanization continues to accelerate, and urban environmental problems become increasingly prominent, among which the urban heat island (UHI) effect is the most significant (Degirmenci et al. 2021). The UHI has a profound impact on urban microclimate, air quality, and public health

(Zak et al. 2020). Therefore, the UHI effect has become the focus of the scientific community, managers, and even the public (Akkose et al. 2021). Numerous studies have shown that the UHI effect is affected by rapid urban development, geographical location, climate change, urban landscape types, and landscape pattern characteristics (El-Hattab et al. 2018). With the further research on the UHI effect, the “cold island” formed by the urban park composed of water and green vegetation is considered to be one of the significant

Responsible Editor: Philippe Garrigues

✉ Jialin Li
lijialin@nbu.edu.cn

Peng Tian
tianpeng@nbu.edu.cn

Ruiliang Pu
rpu@usf.edu

Luodan Cao
caoluodan@nbu.edu.cn

Yongchao Liu
liuyongchao@nbu.edu.cn

Haitao Zhang
2011073029@nbu.edu.cn

¹ Department of Geography and Spatial Information Techniques, Ningbo University, Ningbo 315211, China

² Zhejiang Collaborative Innovation Center & Ningbo Universities Collaborative Innovation Center for Land and Marine Spatial Utilization and Governance Research, Ningbo University, Ningbo 315211, Zhejiang, China

³ Donghai Academy, Ningbo University, Ningbo 315211, China

⁴ School of Geosciences, University of South Florida, Tampa, FL 33620-5250, USA

ways to alleviate the UHI effect and improve the geothermal environment of the urban bureau (Peng et al. 2021). How to adapt and mitigate the UHI effect by using blue-green landscape is an urgent question to be answered.

The urban cold island (UCI) effect develops gradually with the deepening of the research on the UHI effect. Within an UHI, there are scattered areas of cold spots that are significantly cooler than the surrounding environment, a phenomenon known as the UCI (Park et al. 2019). Chinchilla et al. (2021) found that healthy urban trees have a better UCI effect on the surrounding area. Chibuikwe et al. (2018) assessed the UCI effect of green parks on the urban microclimate, and the UCI effect of urban parks has the characteristics of distance attenuation. The spatial form of urban wetland (such as size, shape, and hydrological connectivity) has different UCI effects, and the cooling intensity increases logarithmically with the increase of wetland area (Vidrih and Medved 2013). Green spaces and water bodies in urban parks, or a combination of the two, are the most cardinal sources of cold water in cities. At present, relevant scholars have verified that urban parks could alleviate the UHI phenomenon to a certain extent. The results of Peng et al. (2021) and Chibuikwe et al. (2018) all showed that there was a linear relationship between the land surface temperature (LST) inside urban parks and the distance to the park boundary. Moreover, the UCI effect of urban parks generally includes the evaluation and monitoring of the UCI effect (Lin et al. 2015), the identification of the influencing factors (Peng et al. 2021), and the planning and design of parks under the guidance of the UCI effect (Sugawara et al. 2021). Therefore, how to effectively evaluate the UCI effect of parks is a key step.

In recent years, researchers from different countries have explored the UCI effect of urban parks (Degirmenci et al. 2021). In the identification of urban land surface thermal environment, remote sensing satellites are mainly used to obtain the spatial distribution of land surface temperature (LST) in one year or in a long time series (Taloor et al. 2021; Peres et al. 2018). Data products mainly include Landsat images, MODIS data, Sentinel, Terra, Aqua, environmental satellites, and other data products (Chen 2020; Li et al. 2017). The spatial resolution of thermal infrared sensors ranges from 60 m (ETM+) to 25 km (IASI) (Wang et al. 2020). The TM/ETM+/TIRS sensor on the Landsat-5/7/8 satellite images has a relatively high spatial resolution and short reentry period (16 days) and is widely applied in LST monitoring (Nikam et al. 2016). In the research of quantifying the UCI effect of parks, there are many indicators to evaluate the UCI effect of parks, focusing on the cooling intensity of parks to evaluate the thermal difference between parks and their surrounding environment (Peng et al. 2021; Lin et al. 2015). In addition, scholars added distance variables to measure the UCI effect of parks (Feyisa et al. 2014).

On the basis of analyzing the influencing factors of UCI effect, the structural factors such as park area, perimeter, proportion of green area, and proportion of water area were covered (Chen et al. 2021; Lu et al. 2017).

Although the calculation methods for the UCI effect of urban parks are different, those studies are all focused on exploring the maximum impact distance of park cooling (Sugawara et al. 2021). That is, with the park as the core, analyze the park's maximum cooling area, maximum cooling distance, etc., so as to effectively identify the area with the maximum cooling area affected by the park (Lin et al. 2017). However, some scholars pointed out that the cooling effect of urban parks was continuous rather than discrete in space, so the maximum impact index could not fully describe the spatial changes of urban parks around LST (Toparlar et al. 2018). Thus, it is necessary to evaluate the cooling effect from the perspective of spatial accumulation, that is, to analyze the spatial continuity of cooling effect outside urban parks. Since the geographical distribution of urban parks is directly related to the types of surrounding land use, such as expensive land in urban centers and many high-rise buildings (Li et al. 2021), theme parks and community parks with smaller areas are mostly distributed. The urban suburbs are rich in land resources, and there are many comprehensive parks and ecological parks with large distribution areas (Peng et al. 2021; Lin et al. 2015). Therefore, the UCI effect of urban parks is closely related to the types of surrounding land use, and it is necessary to explore the maximum and accumulative effect of the UCI effect of urban parks from the perspective of different urban park types. Furthermore, the current research on Hangzhou's UCI effect focuses on the impact of urban internal landscape composition and buildings on UHIs or UCIs (Hou and Estoque 2020), and less attention is paid to urban parks with significant cooling effects. Therefore, our study linked the maximum and the accumulative perspectives to comprehensively evaluate the cooling effect of Hangzhou city parks.

Hangzhou, a central city in the Yangtze River Delta region, has been rated as the happiest city in China for 13 consecutive years. However, rapid urbanization and industrialization have put great pressure on the local ecological environment, especially the UHI is the most prominent in Hangzhou (Hou and Estoque 2020; Yue et al. 2019). Given to improve the quality of urban ecological environment and residents' well-being, Hangzhou has made great efforts to build urban parks. Therefore, our study takes the urban area of Hangzhou as the research object and comprehensively measures the cooling effect of urban parks. Specifically, the main objectives of this study are (1) to reveal the spatiotemporal distribution of land cover (LC) changes and UHI effect in Hangzhou, (2) to analyze the UCI effect of urban parks from the perspective of the maximum and accumulative perspectives, and (3) to identify the influencing factors of the UCI effect of

urban parks. It is expected to provide guidance for alleviating the UHI effect of Hangzhou, scientifically planning the rational layout of urban park landscape.

Study area

Hangzhou is located on the southeast coast of China, on the southern edge of the Yangtze River Delta. Hangzhou has a subtropical monsoon climate with four distinct seasons and abundant rainfall (Gou et al. 2019). This research area is the urban area of Hangzhou, including 8 municipal districts (Lin’an and Fuyang districts with extensive forest coverage were screened out) (Fig. 1). Hangzhou is the political, economic, cultural, educational, transportation, and financial center of Zhejiang province and one of the central cities in the Yangtze River Delta city cluster. Hangzhou’s urbanization rate reached 78.5% in 2020. The built-up area increased from 177.18 km² in 2000 to 648.46 km² in 2019, and the population density reached 1100 (person/sq. km).

Data and methods

Analysis framework of UCI effect

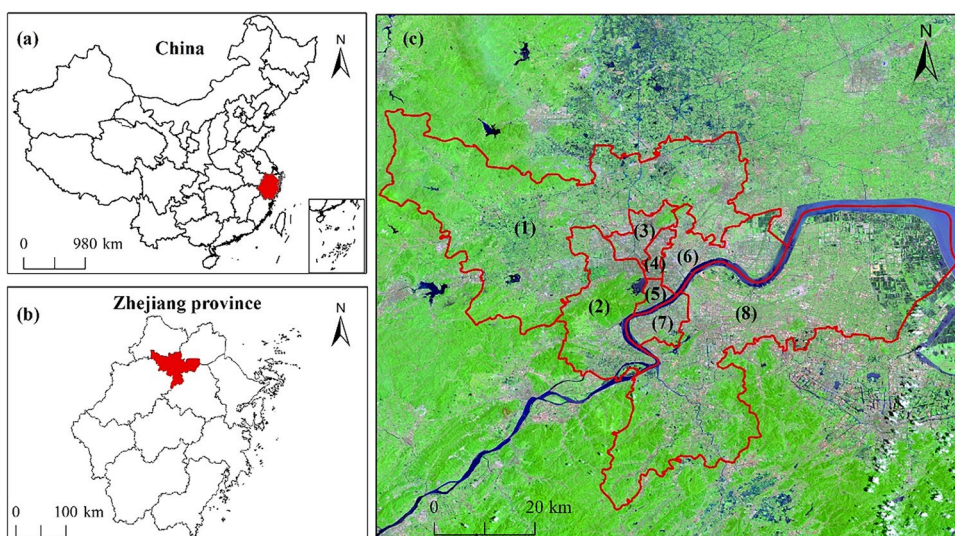
As shown in Fig. 2, the study revealed the UHI effect in the urban area of Hangzhou by using multi-phase Landsat image data. Based on the image of UHI effect in 2020, 30 parks were selected from 248 urban parks based on maximum and accumulative perspectives to analyze the UCI effect of urban parks and explore its influencing factors.

Data and data processing

Our study used Landsat series data to carry out temperature inversion in Hangzhou urban area, and all Landsat data were downloaded from the USGS (<http://glovis.usgs.gov>). The urban area of Hangzhou mainly involved a scene image (119–39). The 21-year images of Landsat-5 TM, Landsat-7 ETM+, and Landsat-8 OLI/TIRS from 2000 to 2020 were selected, and the image time was concentrated at around 12 o’clock in June, July, and August, during which the temperature rose, which could better reflect the LST. However, in the process of practical operation, the images of 2001, 2007, 2012, 2016, 2018, and 2019 were clouded in June to August, so the temperature inversion could not be completed and they were eliminated. Finally, the paper only carried out temperature inversion for the image data of 15 periods. The detailed information of the 15-stage image data is shown in Table A1. In this study, we mainly focused on the changing trend of different grades of UHI. Therefore, the LST layer was divided into five grades (low, sublow, medium, subhigh, and high) by the natural breakpoint method.

To verify the LST results, we combined MOD11A2 product and the LST data recorded on the surface to verify it. The MOD11A2 LST data products (Spatial resolution is 250 m) are collected from LAADS DAAC (<https://ladsweb.modaps.eosdis.nasa.gov>). The measured data on the surface comes from the Hangzhou Meteorological Bureau (<https://www.hzqx.com>). First, we randomly sampled 1500 random points in the study area, obtained 599 effective points (deleted some random points with null values), extracted the values of the inverted LST layer and MOD11A2 layer at each point, and compare the values of the two (Peres et al. 2018). As shown in Fig. 3a, The LST variation trend of Landsat image inversion is basically consistent with that of the MOD11A2 product. In addition, there is a significant correlation between the

Fig. 1 Location of the study area. **a** Location of Zhejiang province in China. **b** Location of the city of Hangzhou in Zhejiang province. **c** Overview of the Hangzhou in a Landsat 8 OLI image taken in 2013 with a false color composite (which three bands (763) vs. RGB). (1) Yuhang District, (2) Xihu District, (3) Gongshu District, (4) Shangcheng, (5) Xiacheng District, (6) Jianggan District, (7) Binjiang District, (8) Xiaoshan District



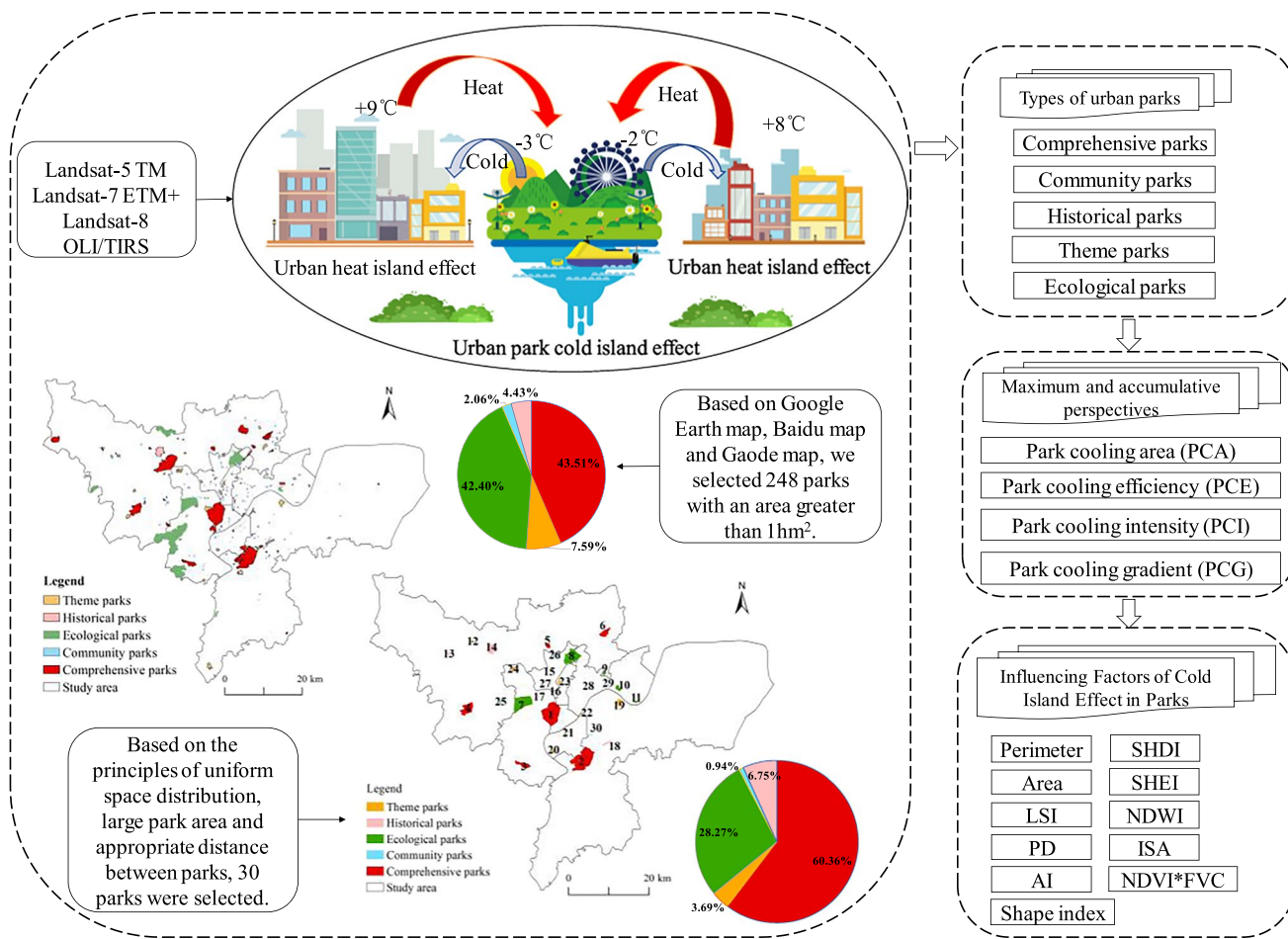
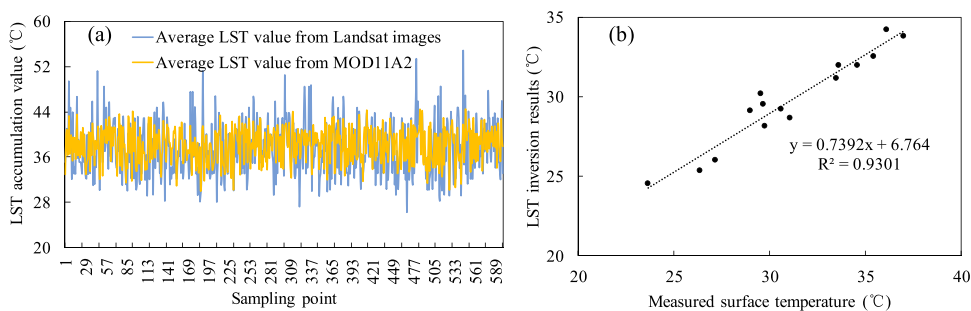


Fig. 2 Research framework of UCI effect

Fig. 3 Comparison of the results of retrieved LSTs from Landsat thermal images with those from MODIS LST product and ground true data (°C)



measured surface temperature and the LST retrieved from the remote sensing images ($R^2=0.9301$) (Fig. 3b), indicating that the results of our study are credible.

Given to reflect the relationship between regional LC and LST, image data in 2000, 2005, 2010, 2015, and 2020 were selected for interpretation. Through the process of radiation and atmospheric correction, study area cutting, supervision, and classification and referring to previous studies and research needs (Xie et al. 2020), we divided it into seven categories: farmland, forest, grassland, water, built-up land,

unused land, and wetland (Fig. A1). Through Google Earth map and field investigation, the interpretation accuracy was more than 85%, which met the research needs.

Hangzhou Municipal People’s Government announced the list of the second batch of parks in Hangzhou in August 2020 (<http://www.hangzhou.gov.cn>), including Shangcheng District (18 parks), Xiacheng District (10 parks), Jianggan District (20 parks), Gongshu District (22 parks), Xihu District (17 parks), Binjiang District (15 parks), Xiaoshan District (16 parks), and Yuhang District (32 parks), a total of

150. There were also many unrecorded urban parks. Based on Google Earth map and Baidu map, we selected 248 parks with an area of more than 1 hm² and drew the spatial distribution map of urban parks in Hangzhou city (Fig. A2). With reference to the classification basis of urban parks in Peng et al. (2021), the classification standard of Hangzhou urban parks is established (Table A2), mainly including comprehensive parks, community parks, historical parks, theme parks, and ecological parks. Given to better analyze the UCI effect of urban parks, we selected 6 representative parks from each type of park (Fig. 4). The principles for selecting parks mainly include (1) uniform spatial distribution, (2) urban parks are well known and representative, (3) urban parks are far away from each other, and the mutual influence is weak. The information of 30 parks is shown in Table A3.

Analysis methods

LST retrieval

In this study, we mainly used a mono-window algorithm developed by Qin et al. (2001) to retrieve the LST. Compared with other radiative transfer equations, the mono-window algorithm directly covers the effects of the atmosphere and the surface in the model equation and is more suitable for long-term series Landsat data. The research method is relatively mature, and the algorithm can be referenced in Qin et al. (2001), Tian et al. (2021), and the supplementary material.

Quantitative evaluation method of thermal effect of LC

To reflect the LST of different LC types, the heat contribution index (Hi), weighted heat unit index (D1), and regional weighted heat unit index (D2) for each LC type were calculated. For the calculation formula, refer to Du et al. (2020) and the supplementary material.

UCI effect measurement in urban parks

Since the resolution of the Landsat imagery data is 30 m, we generated 10 buffers of 30 m width from the park boundary (total buffer width is 300 m). Then, we further set the buffer distance as the independent variable *X*, set the average LST in each buffer as the dependent variable *T*, and establish the functional relationship between the buffer and the LST. After many curve fitting analysis of the function, the cubic polynomial can best express the relation (average *R*² > 0.900) (Peng et al. 2021). The cubic polynomial function *T*(*x*) was established as follows:

$$T(x) = ax^3 + bx^2 + cx + d \tag{1}$$

Urban parks are the center of the UCI effect. The LST tends to grow as the buffer distance increases. As the distance continues to expand, the growth rate of the LST tends to decrease and shrinks to 0, and the first derivative of the function *T*(*x*) is 0 at this point, known as the first turning point of the LST curve (Fig. 5). This point reflects the first decrease in LST as the buffer increases. Beyond the first turning point, the cooling effect of the park on the surrounding area diminishes. The LST of the turning point is defined

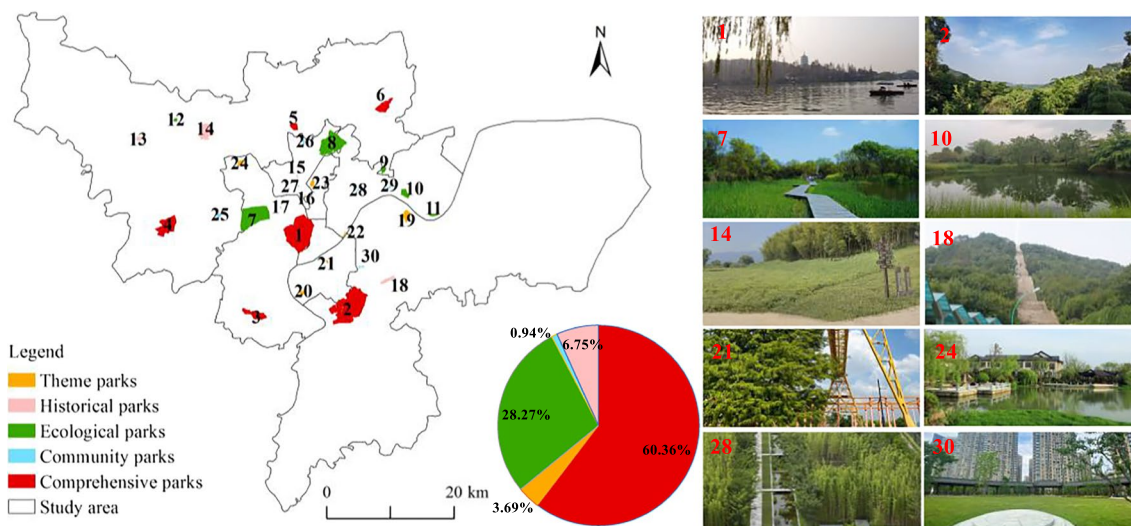
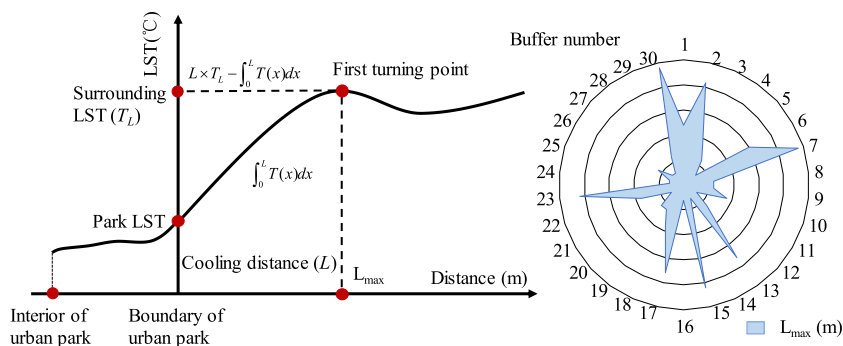


Fig. 4 Distribution of 30 selected parks and area ratio of different types of parks. Note: 1 West Lake Scenic Area, 2 Xianghu National Tourist Resort, 7 Xixi National Wetland Park, 10 Qiantang Ecologi-

cal Park, 14 Liangzhu Ancient City Relics Park, 18 Beishan Park, 21 Industrial Heritage Park, 24 Hangzhou Tianjing Aquatic Botanical Garden, 28 Yangliu County West Park, 30 Beitang Park

Fig. 5 Schematic diagram of park cooling process and the maximum cooling distance of 30 parks



as the surrounding LST of the urban parks, and the distance from the first turning point to the park boundary is defined as the maximum cooling distance L_{\max} . Specific indicators (park cooling area, PCA; park cooling efficiency, PCE; park cooling intensity, PCI; and park cooling gradient, PCG) are introduced in the supplementary material. Among them, PCA and PCE reveal the UCI effect of urban parks from a maximum perspective, while PCI and PCG reflect an accumulative perspective.

Factors influencing UCI effect of urban parks

To analyze the influencing factors of UCI effect, we must start from the perspective of park and its surrounding environment. According to the previous research experience, it generally includes the landscape pattern of the park (internal structure), the landscape site of the park (landscape connectivity), and the landscape pattern around the urban park (Sun and Chen 2012). On the landscape scale, we selected perimeter, area, shape index, landscape shape index (LSI), patch density (PD), aggregation index (AI), Shannon's diversity index (SHDI), and Shannon's evenness index (SHEI) of urban parks to test how the spatial configuration of parks affects the cooling effect. The meanings and formulas of LSI, PD, AI, SHDI, and SHEI landscape indexes can refer to Liu et al. (2018). Vegetation coverage reflects regional vegetation coverage and has a significant cooling effect on LST. However, only NDVI and vegetation coverage (FVC) could not well represent vegetation factors, so they should be combined to comprehensively consider the vegetation coverage and greenness of parks (Peng et al. 2021). In addition, the impervious surface index (ISI) represented by the construction land and the normalized water index (NDWI) represented by the lake also have a significant effect on the LST. The specific calculation methods of various indices are relatively mature; refer to Xu (2006, 2010), McFEETERS (1996), and Peng et al. (2020, 2021, 2017). Finally, we input 11 indicators of perimeter, area, shape index, LSI, PD, AI, SHDI, SHEI, NDVI*FVC, ISA, and NDWI and 4 indicators of PCA, PCE, PCI, and PCG into SPSS 25 for correlation

analysis, so as to analyze the influencing factors of UCI effect in parks.

Results

Characteristics of LC and thermal environment changes

Contribution of LC types to UHI effect

LC in Hangzhou has changed drastically from 2000 to 2020 (Fig. A3 and Table A4). The area of built-up land increased by 116.44% in 20 years, mainly from farmland, forest, and water area. It obviously showed that Hangzhou had experienced a rapid urbanization process. With the acceleration of urbanization, the UHI effect has also intensified. As shown in Fig. 6, the high-value areas of the UHI effect were concentrated in the city center, and the range of high-value areas continues to expand. From 2000 to 2006 (e.g., Fig. 6a–f.), the high-value areas of the UHI effect were concentrated in the north of Qiantang River. After 2008 (e.g., Fig. 6g–o), the high-value area of the UHI effect continued to spread to the south of the Qiantang River, indicating that the city continued to develop to the south of Qiantang River, which intensified the UHI effect in the southern region.

Although the average LST of LC types was different, they all showed an upward trend, indicating the deepening of Hangzhou's UHI effect (Table 1). The order of the average LST of land types was built-up land > farmland > unused land > forest > grassland > water > wetland. The average LST of built-up land and farmland increased the fastest, increasing by 15.93 °C and 15.8 °C, respectively, from 2000 to 2020. The H_i of built-up land and farmland was the largest. The H_i of built-up land was increasing continuously (Fig. A4), from 35.90% in 2000 to 62.66% in 2020, indicating that construction land aggravated the regional UHI effect. By analyzing the D1 and D2 of different LC types, it showed that the land area with higher LST in built-up land and farmland accounted for a larger proportion.

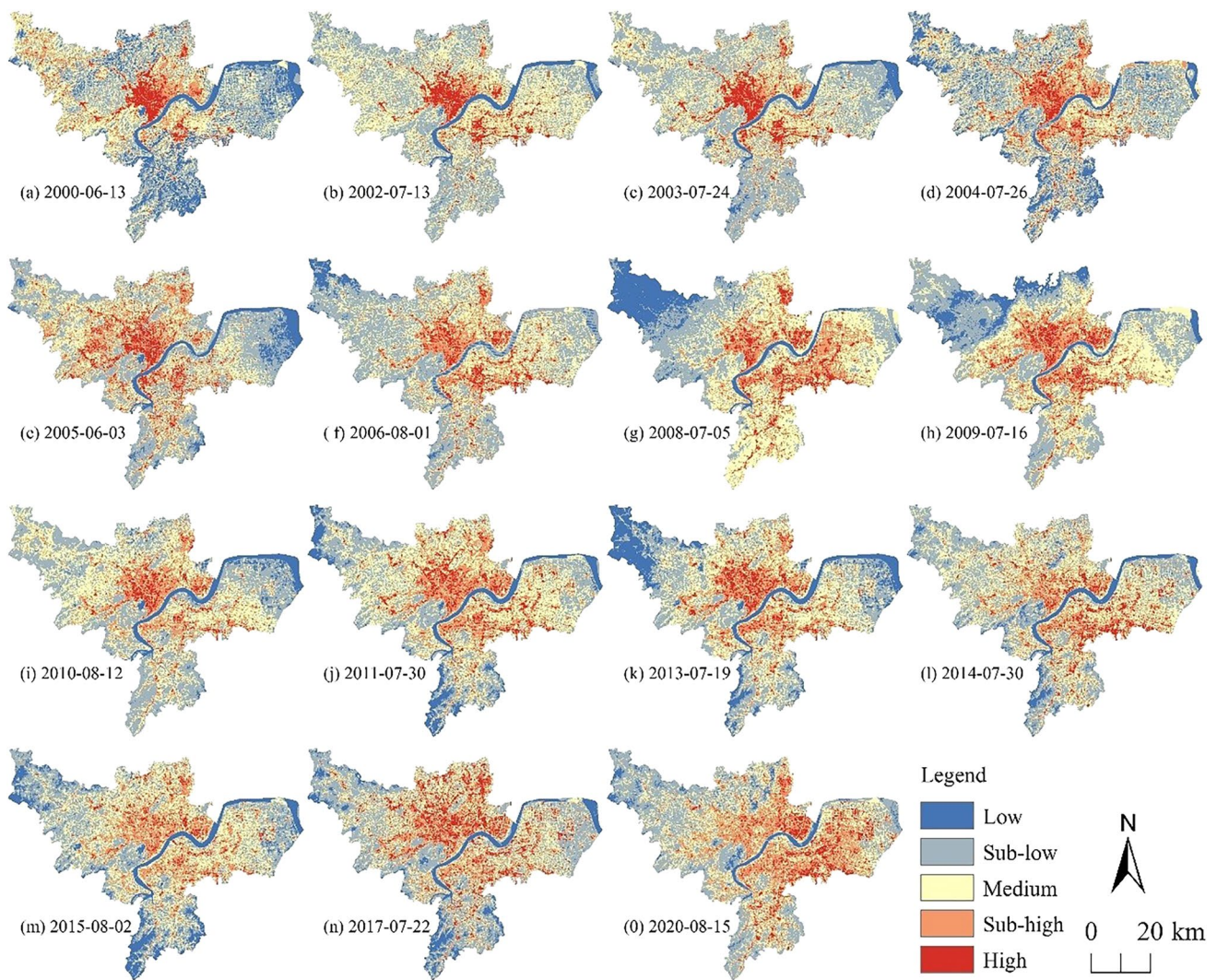


Fig. 6 Spatiotemporal distribution characteristics of LST

Table 1 Average LST variation of different LC types (°C)

LC types	2000	2005	2010	2015	2020
Farmland	24.66	34.10	35.81	39.84	40.46
Forest	25.06	32.86	34.27	36.18	36.50
Grassland	24.92	32.37	33.70	36.24	37.62
Water	22.40	29.93	32.29	35.05	36.33
Built-up land	28.02	36.31	39.15	44.37	43.95
Unused land	27.85	33.94	35.68	38.62	38.29
Wetland	21.58	28.33	31.01	34.84	38.18

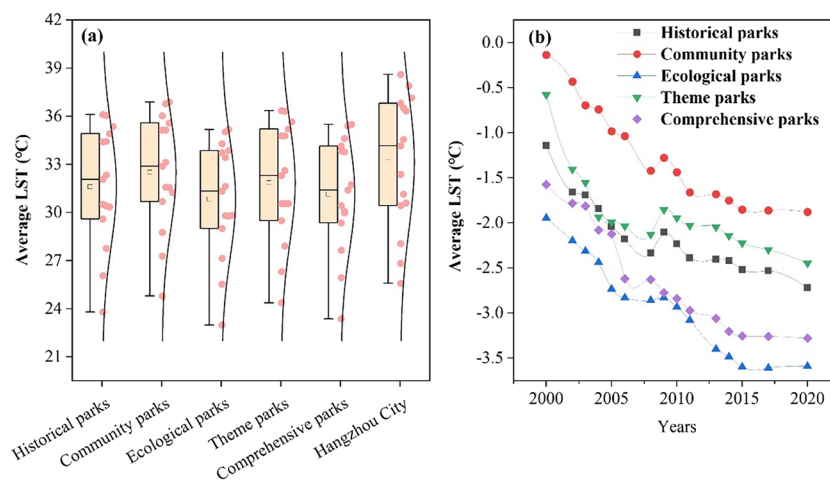
In summary, artificial land, mainly built-up land and farmland, contributed the most to the UHI effect, while ecological land, mainly forest, grassland, and waters, had the lowest contribution to the UHI effect. It indicated that the ecological land within the city presented a significant UCI

effect, and the construction of urban parks had considerable ecological significance.

The cooling effect of multi-urban park types

Given to further analyze the cooling effect of ecological land, we took 248 parks in the urban area as the research object to reveal the UCI effect of parks. The average LST inside the urban parks was lower than the average LST in Hangzhou (Fig. 7a), where Hangzhou city > community park > theme parks > historical parks > comprehensive parks > ecological parks. The difference value increased slightly in 2009, mainly due to the acceleration of urbanization in Hangzhou city (Fig. 7b), which led to a rapid increase in the average LST. In some areas, there were no parks in the early stage and then urban parks were built. With the deepening of the UHI effect, the difference of average LST

Fig. 7 Statistics of average LST of different types of urban parks. **a** Average LST of Hangzhou city and its urban parks from 2000 to 2020. **b** The difference of average LST between the urban parks and Hangzhou city from 2000 to 2020



between the urban parks and the Hangzhou city was also expanding, indicating that the UCI effect of urban parks was more prominent after the construction and reflecting the necessity and significance of building urban parks.

Cooling effects of urban parks from maximum and accumulative perspectives

The spatial distribution of UCI effect

Given to further analyze the UCI effect of the park, we only selected the 2020 UHI effect image and 30 representative parks for analysis. On August 15, 2020, the maximum LST in Hangzhou urban area reached 54.85 °C, the minimum was 17.15 °C, and the average was 37.61 °C. Spatially, the high LST areas were concentrated in the city center (Fig. 6 o), distributed in the central and eastern regions of commercial areas, residential areas, public squares, and other built-up land intensive areas, while the northwest and southwest corners of the LST were relatively low. In the urban center, there were also some low LST zones, corresponding to urban parks, rivers, lakes, and other ecological land.

The Getis-Ord G_i^* spatial hot spot analysis tool based on ArcGIS10.5 software reflects the hot and cold spot distribution of the LST in the local space, which can effectively highlight the spatial heterogeneity of LST in the urban area of Hangzhou. The hot and cold spots were defined as the high or low LST tended to cluster in space (Tran et al. 2017). As shown in Fig. 8a, the superposition area of 30 parks and cold spot area (with over 90%, 95%, and 99% confidence) accounted for 83.54% of the total area, indicating that the cooling effect of urban parks in downtown Hangzhou was outstanding. To further illustrate the cooling effect of parks, we selected three major parks in Hangzhou for analysis. The types of West Lake Scenic Area Park (1), Xixi National Wetland Park (7), and Beishan Park (18) are comprehensive parks, ecological parks, and historic parks (Fig. 8b–e). The

surface temperature within their range was lower than that of the surrounding ones and had a certain cooling impact on the surrounding area.

By comparing the average LST inside 30 parks with the average LST of surrounding (L_{max}) (Fig. A5), the average LST inside the parks was lower than the average LST of the surrounding environment (by 2.47 °C) and was also lower than the average LST in Hangzhou (by 0.73 °C). It also indicated that urban parks had a significant UCI effect, which could reduce the surrounding LST.

UHI mitigate by urban parks in terms of maximum and accumulative perspectives

As shown in Fig. 9, we calculated four cooling indices for 30 parks. The PCA of comprehensive park (1–6) and ecological park (7–12) was obviously larger than that of other park types, indicating that the cooling area of comprehensive park and ecological park was larger. The area of green infrastructure in comprehensive parks and ecological parks was relatively large, such as forest, grassland, and water landscape, so the PCA was larger than other park types. Community parks (25–30) had the highest PCE, indicating that they had an effective cooling effect on the surrounding features. Due to limited urban land resources, urban planners have to increase the density and height of buildings to meet the living needs of the growing population, which intensifies the regional UHI effect. The community parks are mostly distributed in residential areas with dense construction, generally with small lakes, green spaces, rivers, and other landscapes. Although community parks are relatively small, the LST of community parks is much lower than that of residential areas, making community parks the center of the regional UCI. As a result, community parks cool a larger residential area with a smaller area, making their PCE particularly outstanding.

Fig. 8 Spatial patterns of a cold-hot spot areas and UHI cavity inside the b, c Beishan Park and d, e West Lake Scenic Area Park and Xixi National Wetland Park

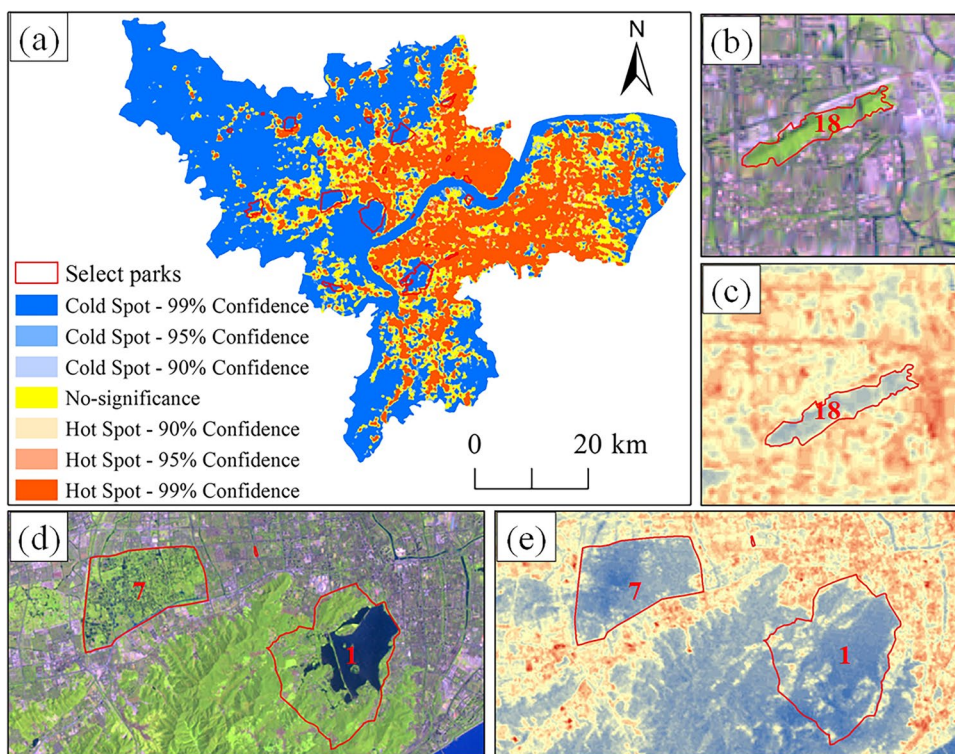
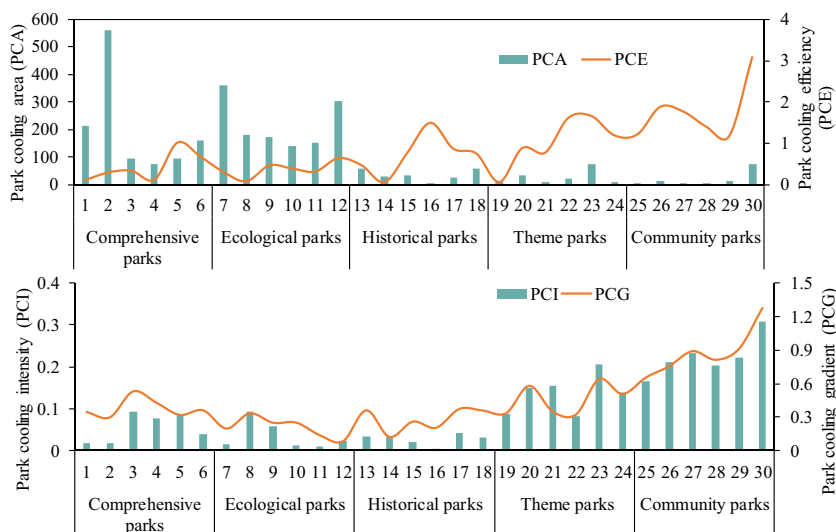


Fig. 9 Cooling indexes of the 30 urban parks



In addition, the PCI and PCG of theme parks and community parks are significantly higher than those of other types of parks. The UHI effect is more prominent in densely built areas, such as urban centers and residential areas, while theme parks and community parks are located close to these areas. Therefore, theme parks and community parks present intensive and high heat absorption characteristics, and the ratio of the reduced regional temperature to the regional original temperature is slightly larger

than other types of parks, especially large comprehensive parks and ecological parks distributed in the periphery of cities. The building density around other types of parks is lower than that of theme parks and community parks, showing a broad low heat absorption process. The residents’ perception of LST reduction in such parks is slightly lower than that of urban parks near the center of the UHI. Therefore, the theme parks and community parks in the urban area have a stronger cumulative effect of UCI effect.

Influencing factors of urban park cooling effects

The correlation coefficient between the UCI index of the park and the influencing factors is shown in Table 2. PCA was significantly positively correlated with the perimeter and area of the park, and the correlation coefficients were 0.694 and 0.697 respectively ($P < 0.01$). It showed that the larger the area and perimeter of the park, the wider the influence range on the surrounding LST. For example, the maximum cooling distance of Xixi Wetland Park and Xianghu National Tourism Resort reaches 240 and 210 m, respectively. There was a significant negative correlation between PCE and park perimeter and area, and the correlation coefficients were -0.488 and -0.748 , respectively ($P < 0.01$). It showed that the area of the park did not determine the cooling efficiency of the park, which was most obvious in the community park. For example, Beitang Park in the community park had an area of only 6.75 hm², but the maximum distance of the cooling area (S_{\max}) reached 240 m.

PCE maintained a negative correlation with park shape index ($r = -0.789$, $P < 0.01$). It showed that the smaller the shape index of the park, the closer the shape of the park was to a circle, which was not conducive to the PCE. LSI, SHDI, and SHEI showed significant positive correlation with PCA and significant negative correlation with PCE, indicating that the more complex the park boundary was and the more landscape types were, the more effective the park UCI effect would be. PD reflected the fragmentation degree of the park. The larger PD was, the more fragmented the landscape patches were, which was not conducive to the UCI effect of the park. Therefore, PD was negatively correlated with PCA and PCE. AI index reflected the concentration degree of the park landscape, and the correlation coefficients were all low. PCA was positively correlated with NDVI*FVC

and NDWI, and the correlation coefficients were 0.612 and 0.553, respectively ($P < 0.01$). The higher the vegetation coverage and water coverage, the better the cooling effect of parks, especially most parks in Hangzhou owned lakes, and the better the cooling efficiency of parks (the correlation coefficient between PCE and NDWI was 0.649, $P < 0.01$). The larger the impervious surface area of the park was, the less conducive to PCA and PCE, and the correlation coefficients were negative.

PCI, PCG, and NDVI*FVC were significantly correlated, and the correlation coefficients were 0.576 and 0.564, respectively ($P < 0.01$). The larger the NDVI*FVC, the higher the vegetation coverage in the park, so the greater the ratio of LST reduction to the total LST around, which marked the cooling process more intense, resulting in higher PCI and PCG. In addition, the increased greening of the park will lead to frequent air exchanges inside and outside the park, thereby contributing to the growth of PCI and PCG. PCI and PCG had a low correlation with other influencing factors and did not pass the significance test.

Discussion

Quantitative assessment of spatial continuity of cooling effects in urban parks

How to characterize the spatial continuous changes of UCI plays an extremely cardinal role quantitatively and effectively in revealing the spatial distribution of UCI effects. In the early stage, the spatial differentiation of UCI effect was reflected by field temperature measurement at different locations in the city (Yan et al. 2018), but the cost of time and money was higher, and the field observation was greatly affected by weather. With the rise of “3S” technology, the UCI effect revealed by remote sensing images is more popular and common (Cheval et al. 2020; Estoque and Murayama 2017), and the establishment of different levels of buffer zones can better reflect the spatial heterogeneity of UCI effect. Although the UCI effect of parks is different, the maximum cooling distance of most parks is less than 1000 m (Peng et al. 2021). Therefore, predecessors' research buffers mostly used 10–30 buffers, each 30 m wide, and the workload was average and easy to operate. This has also been widely used in the analysis of the buffer zone of the park's UCI effect in parks.

In this study, we established a 300 m wide buffer zone based on the park boundary to analyze the maximum cooling distance of 30 parks. When the article initially selected the buffer width, we established the buffer widths of 300 m (10 buffers), 600 m (20 buffers), and 900 m (30 buffers), respectively, as shown in Fig. 10. The inflection point distance of the function describing the distance-LST relationship

Table 2 Correlation coefficient between UCI index and various influencing factors

Characteristics	PCA	PCE	PCI	PCG
Perimeter	0.694**	-0.488**	0.254	0.247
Area	0.697**	-0.748***	0.142	0.132
Shape index	0.573**	-0.789***	-0.014	-0.002
LSI	0.535**	-0.630**	0.105	0.100
PD	-0.644**	-0.592**	-0.130	-0.119
AI	0.090	-0.437**	-0.208	-0.213
SHDI	0.672**	-0.466**	0.286	0.271
SHEI	0.669**	-0.446**	0.295	0.279
NDVI*FVC	0.612**	0.043	0.576**	0.564**
ISA	-0.612**	-0.528**	-0.063	-0.047
NDWI	0.553**	0.649**	0.011	-0.004

***Significance at 0.001 level

**Significance at 0.01 level

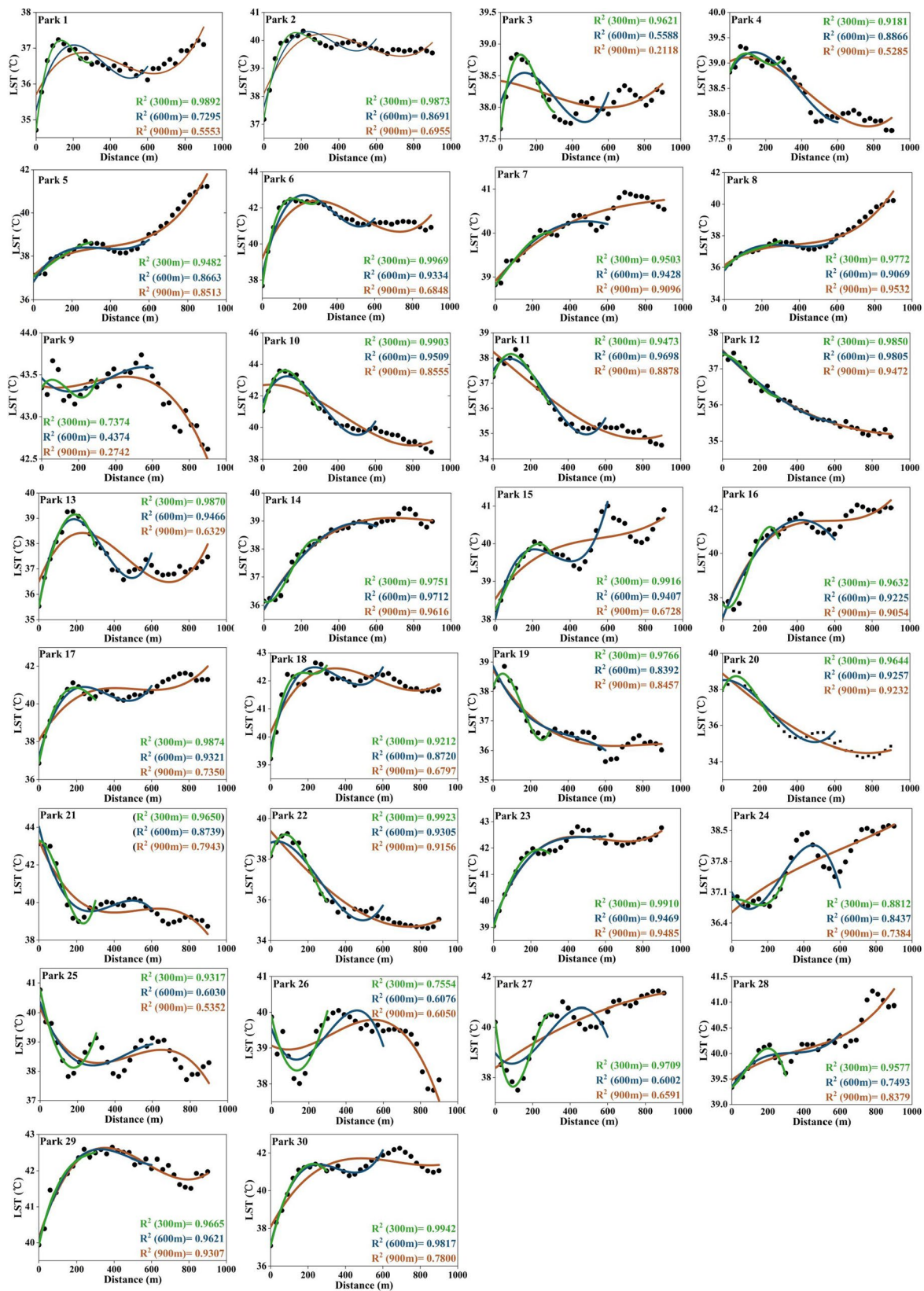


Fig. 10 Cubic polynomial relationships between LST and the distance from each of the 30 urban parks

under different buffer widths was different. The larger the buffer width was, the statistical description of this relationship tended to get worse (R^2 value decreased). Among the 30 parks, 29 parks showed the largest R^2 value at 300 m. Only Park 11 behaved the largest R^2 value at 600 m. In addition, among the 30 parks, only Xixi Wetland Park and Beitang Park had the maximum cooling distance of 240 m, while the other parks had the maximum cooling distance of far less than 300 m. In summary, when the buffer was 300 m, the data mathematically fits better than the 600 m and 900 m buffer widths. Therefore, we chose 300 m for the buffer width.

The cooling effect of urban park types and urban planning management

Urban UCIs formed by urban parks composed of landscapes such as water bodies and green vegetation are a significant means to improve the local urban thermal environment (Xu et al. 2017). Due to the abnormal shortage of urban land resources caused by rapid urbanization, how to maximize the UCI effect in the precious park landscape and realize the high benefits of improving the urban thermal environment has become one of the ecological problems to be urgently solved. Numerous studies have shown that the cooling of urban parks is a nonlinear process (Peng et al. 2021). Planners must fully understand the maximum cooling distance of urban parks and cannot ignore the spatial continuity of cooling effects.

The cooling effect of different types of parks is different, and the cooling effect of ecological park is the most obvious in our study. The order of the average LST in each type of park is ecological parks (33.90 °C) > comprehensive parks (34.79 °C) > historical parks (35.67 °C) > theme parks (36.76 °C) > community parks (38.72 °C). Therefore, if urban park planning is committed to building public spaces that benefit more residents, ecological parks should be given priority, because the PCA of this park is prominent. Furthermore, the ecological park should be built near residential areas and the city center to better utilize the accumulative cooling effect of urban parks (PCI and PCG). From the perspective of cooling efficiency, community parks are undoubtedly the best choice because they occupy smaller areas, have lower costs, and show an outstanding accumulative cooling effect. In addition, theme parks and historical parks, through the design of specific landscape to provide urban residents with cultural and entertainment services, increasing their ecological landscape area, could not only play the leisure culture and entertainment service functions but also could effectively alleviate the UHI effect. If the cost of time and money is sufficient, it may be a good choice to build a comprehensive park, which has a large PCA (Peng et al. 2021). However, the comprehensive park also needs to improve the cooling efficiency and increase its

cumulative cooling capacity. Moreover, it is necessary to consider the potential negative effects of green infrastructure in park planning, such as the impact of increased emissions of volatile organic compounds and pollen on human health and how wild animals and plants coexist harmoniously with human society (Parmes et al. 2020).

Based on the analysis of the factors influencing the cooling effect of urban parks in our study, given to achieve the best cooling effect of urban parks, attention should be paid to the area and complexity of landscape shape of urban parks when designing urban parks, and the UCI effect can be enhanced by appropriate expansion of parks. Green spaces absorb solar radiation through photosynthesis and transpiration and reduce surface temperature through the shading function of plants (Sugawara et al. 2021). We should consider increasing the area of park green space and repair the relatively scattered green space patches to form large continuous green space landscape as far as possible, which could not only enhance the cooling effect from the maximum and accumulative perspectives but also enhance the esthetic value of landscape. At the same time, the cooling effect of the water area around the park is significant, and the lake landscape can be appropriately increased. In addition, control the area of construction land in the park and reduce the area of impervious surface, such as roads, pavilions, and artificial leisure facilities.

Limitations and prospect

Based on the multi-period remote sensing image data, our study revealed the spatiotemporal distribution characteristics of the UCI effect in the urban area of Hangzhou. The spatial continuity of the maximum index and the accumulative index were comprehensively considered. However, our study also has some limitations. Firstly, the study revealed that the data source of UHI effect in Hangzhou urban area was Landsat dataset with medium spatial resolution, which may have a certain influence on the results (Peng et al. 2021). Future research should increase the use of high-resolution images to improve the accuracy of data and results. Then, our research only considers daytime conditions, but the cooling effect of urban green space will be extremely different in the day and night cycle. For example, in the daytime, the green space is mainly used as a cold source to cool the surroundings, while at night, the green space (mainly water) cools slowly and acts as a heat source for heat preservation. Therefore, we should strengthen the research on the characteristics of the surface temperature change of the green space system at night and its impact on the surroundings. In addition, the paper only used the LST data in the summer of 2020 to analyze the UCI of urban parks. In subsequent studies, it will be considered to increase the temporal characteristics of

the UCI effect of urban parks in different seasons of spring, summer, autumn, and winter.

Moreover, since the internal landscape of the park is relatively detailed, it is difficult to identify all features such as signage, trails, trash cans, and resting tables and chairs based on medium-resolution images. Therefore, future research can combine high-scoring images, street scene images, field surveys, etc. to subdivide the internal landscape of the park, to explore the role of UCIs played by various landscapes in the park, and further guide the planning and layout of the park. Finally, there are many influencing factors for the UCI in the park, and wind factors, tree species types, vegetation accumulation, and other appropriate landscape pattern indexes can be added for analysis.

Conclusions

Explaining the UCI effect of urban parks could provide practical guidance for the planning and management of urban parks, thus alleviating the UHI effect and improving the happiness of urban residents. Based on Landsat image data for many years, our study revealed the changes of LC and UHI effect in Hangzhou urban area. 30 urban parks were selected to measure the UCI of parks by integrating maximum and accumulative perspectives. The influencing factors of the UCI effect of different types of parks were analyzed, which enriched the research on the cooling process and influencing factors of parks. The main conclusions were as follows. (1) The urban area of Hangzhou had experienced rapid urbanization from 2000 to 2020, and the built-up land area increased by 116.44%, which intensified the UHI effect. The LST of built-up land and farmland increased by 15.93 °C and 15.80 °C during 2000 to 2020, respectively, making the built-up land and farmland the largest contribution to the regional UHI effect. (2) Urban parks played a significant role in alleviating the UHI effect, and the UCI effects of different parks were different. Among them, ecological parks and comprehensive parks owned the largest PCA, while community parks and theme parks retained the highest PCE, PCI, and PCG. (3) PCA maintained a significant positive correlation with perimeter, area, SHDI, and SHEI, and the correlation coefficients were all greater than 0.65 ($P < 0.01$), while PCA maintained a significant negative correlation with PD and ISA, and the correlation coefficients were all less than -0.60 ($P < 0.01$). PCE showed a negative correlation with influencing factors, while PCI and PCG showed low correlations with each influencing factor.

Supplementary Information The online version contains supplementary material available at <https://doi.org/10.1007/s11356-023-28088-6>.

Acknowledgements We would like to thank the anonymous reviewers and editors for their valuable comments and suggestions.

Author contribution Conceptualization: PT and LC. Methodology: PT, JL, and LC. Writing—original draft preparation: PT and YL. Writing—review and editing: RP and HZ. All authors contributed to the study conception and design. All authors have read and agreed to the published version of the manuscript.

Funding This research was supported by the National Natural Science Funded project (42276234, 41976209), Natural Science Foundation of Zhejiang Province (LQ20D010006), and Ningbo Natural Science Foundation (2022J092).

Data availability The data can be available on request.

Declarations

Ethics approval Not applicable.

Consent to participate Not applicable.

Consent for publication Not applicable.

Competing interests The authors declare no competing interests.

References

- Akkose G, Meral Akgul C, Dino IG (2021) Educational building retrofit under climate change and urban heat island effect. *J Build Eng* 40:102294. <https://doi.org/10.1016/j.jobte.2021.102294>
- Chen X, Wang Z, Bao Y (2021) Cool island effects of urban remnant natural mountains for cooling communities: a case study of Guiyang, China. *Sustain Cities Soc* 71:102983. <https://doi.org/10.1016/j.scs.2021.102983>
- Chen T-L (2020) Mapping temporal and spatial changes in land use and land surface temperature based on MODIS data. *Environ Res* 110424. <https://doi.org/10.1016/j.envres.2020.110424>
- Cheval S, Popa A-M, Şandric I, Ioja I-C (2020) Exploratory analysis of cooling effect of urban lakes on land surface temperature in Bucharest (Romania) using Landsat imagery. *Urban Clim* 34:100696. <https://doi.org/10.1016/j.uclim.2020.100696>
- Chibuiki EM, Ibukun AO, Abbas A, Kunda JJ (2018) Assessment of green parks cooling effect on Abuja urban microclimate using geospatial techniques. *Remote Sens Appl : Soc Environ* 11:11–21. <https://doi.org/10.1016/j.rsase.2018.04.006>
- Chinchilla J, Carbonnel A, Galleguillos M (2021) Effect of urban tree diversity and condition on surface temperature at the city block scale. *Urban For Urban Green* 60:127069. <https://doi.org/10.1016/j.ufug.2021.127069>
- de Peres LF, de Lucena AJ, Rotunno Filho OC, de França JRA (2018) The urban heat island in Rio de Janeiro, Brazil, in the last 30 years using remote sensing data. *Int J Appl Earth Observ Geoinform* 64:104–116. <https://doi.org/10.1016/j.jag.2017.08.012>
- Degirmenci K, Desouza KC, Fieuw W et al (2021) Understanding policy and technology responses in mitigating urban heat islands: a literature review and directions for future research. *Sustain Cities Soc* 70:102873. <https://doi.org/10.1016/j.scs.2021.102873>
- Du J, Xiang X, Zhao B, Zhou H (2020) Impact of urban expansion on land surface temperature in Fuzhou, China using Landsat imagery. *Sustain Cities Soc* 61:102346. <https://doi.org/10.1016/j.scs.2020.102346>
- El-Hattab M, Amany SM, Lamia GE (2018) Monitoring and assessment of urban heat islands over the Southern region of Cairo Governorate, Egypt. *Egypt J Remote Sens Space Sci* 21:311–323. <https://doi.org/10.1016/j.ejrs.2017.08.008>

- Estoque RC, Murayama Y (2017) Monitoring surface urban heat island formation in a tropical mountain city using Landsat data (1987–2015). *ISPRS J Photogramm Remote Sens* 133:18–29. <https://doi.org/10.1016/j.isprsjprs.2017.09.008>
- Feyisa GL, Dons K, Meilby H (2014) Efficiency of parks in mitigating urban heat island effect: an example from Addis Ababa. *Landsc Urban Plan* 123:87–95. <https://doi.org/10.1016/j.landurbplan.2013.12.008>
- Gou R, Zhao X, Bu Y et al (2019) Dynamic study on the heat island effect and landscape pattern in urban area of Hangzhou. *Res Soil Water Conserv* 26:316–322+329
- Hou H, Estoque RC (2020) Detecting cooling effect of landscape from composition and configuration: an urban heat island study on Hangzhou. *Urban For Urban Green* 53:126719. <https://doi.org/10.1016/j.ufug.2020.126719>
- Li C, Zheng Y, Wu Y (2017) Recovering missing pixels for Landsat ETM + SLC-off imagery using HJ-1A /1B as auxiliary data. *Int J Remote Sens* 38:3430–3444. <https://doi.org/10.1080/01431161.2017.1295484>
- Li J, Zhan W, Hong F et al (2021) Similarities and disparities in urban local heat islands responsive to regular-, stable-, and counter-urbanization: a case study of Guangzhou, China. *Build Environ* 199:107935. <https://doi.org/10.1016/j.buildenv.2021.107935>
- Lin W, Yu T, Chang X et al (2015) Calculating cooling extents of green parks using remote sensing: method and test. *Landsc Urban Plan* 134:66–75. <https://doi.org/10.1016/j.landurbplan.2014.10.012>
- Lin P, Lau SSY, Qin H, Gou Z (2017) Effects of urban planning indicators on urban heat island: a case study of pocket parks in high-rise high-density environment. *Landsc Urban Plan* 168:48–60. <https://doi.org/10.1016/j.landurbplan.2017.09.024>
- Liu Y, Liu Y, Li J et al (2018) Evolution of landscape ecological risk at the optimal scale: a case study of the open coastal wetlands in Jiangsu, China. *Int J Environ Res Public Health* 15:1691. <https://doi.org/10.3390/ijerph15081691>
- Lu J, Li Q, Zeng L et al (2017) A micro-climatic study on cooling effect of an urban park in a hot and humid climate. *Sustain Cities Soc* 32:513–522. <https://doi.org/10.1016/j.scs.2017.04.017>
- McFEETERS SK (1996) The use of the normalized difference water index (NDWI) in the delineation of open water features. *Int J Remote Sens* 17:1425–1432. <https://doi.org/10.1080/01431169608948714>
- Nikam BR, Ibragimov F, Chouksey A et al (2016) Retrieval of land surface temperature from Landsat 8 TIRS for the command area of Mula irrigation project. *Environ Earth Sci* 75:1169. <https://doi.org/10.1007/s12665-016-5952-3>
- Park CY, Lee DK, Asawa T et al (2019) Influence of urban form on the cooling effect of a small urban river. *Landsc Urban Plan* 183:26–35. <https://doi.org/10.1016/j.landurbplan.2018.10.022>
- Parmes E, Pesce G, Sabel CE et al (2020) Influence of residential land cover on childhood allergic and respiratory symptoms and diseases: evidence from 9 European cohorts. *Environ Res* 183:108953. <https://doi.org/10.1016/j.envres.2019.108953>
- Peng J, Liu Q, Xu Z et al (2020) How to effectively mitigate urban heat island effect? A perspective of waterbody patch size threshold. *Landsc Urban Plan* 202:103873. <https://doi.org/10.1016/j.landurbplan.2020.103873>
- Peng J, Dan Y, Qiao R et al (2021) How to quantify the cooling effect of urban parks? Linking maximum and accumulation perspectives. *Remote Sens Environ* 252:112135. <https://doi.org/10.1016/j.rse.2020.112135>
- Qin ZH, Zhang MH, Karnieli A, Berliner P (2001) Mono-window algorithm for retrieving land surface temperature from Landsat TM6 data. *Acta Geographica Sinica*, 56(4), 456–466
- Sugawara H, Narita K, Mikami T (2021) Vertical structure of the cool island in a large urban park. *Urban Clim* 35:100744. <https://doi.org/10.1016/j.uclim.2020.100744>
- Sun R, Chen L (2012) How can urban water bodies be designed for climate adaptation? *Landsc Urban Plan* 105:27–33. <https://doi.org/10.1016/j.landurbplan.2011.11.018>
- Taloor AK, Drinder Singh M, Chandra Kothiyari G (2021) Retrieval of land surface temperature, normalized difference moisture index, normalized difference water index of the Ravi basin using Landsat data. *Appl Comput Geosci* 9:100051. <https://doi.org/10.1016/j.acags.2020.100051>
- Tian P, Li J, Cao L et al (2021) Assessing spatiotemporal characteristics of urban heat islands from the perspective of an urban expansion and green infrastructure. *Sustain Cities Soc* 74:103208. <https://doi.org/10.1016/j.scs.2021.103208>
- Toparlar Y, Blocken B, Maiheu B, van Heijst GJF (2018) The effect of an urban park on the microclimate in its vicinity: a case study for Antwerp, Belgium. *Int J Climatol* 38:e303–e322. <https://doi.org/10.1002/joc.5371>
- Tran DX, Pla F, Latorre-Carmona P et al (2017) Characterizing the relationship between land use land cover change and land surface temperature. *ISPRS J Photogramm Remote Sens* 124:119–132. <https://doi.org/10.1016/j.isprsjprs.2017.01.001>
- Vidrih B, Medved S (2013) Multiparametric model of urban park cooling island. *Urban For Urban Green* 12:220–229. <https://doi.org/10.1016/j.ufug.2013.01.002>
- Wang C, Zhan W, Liu Z et al (2020) Satellite-based mapping of the Universal thermal climate index over the Yangtze River Delta urban agglomeration. *J Clean Prod* 277:123830. <https://doi.org/10.1016/j.jclepro.2020.123830>
- Xie Q, Sun Q, Ouyang Z (2020) Monitoring spatiotemporal evolution of urban heat island effect and its dynamic response to land use/land cover transition in 1987–2016 in Wuhan, China. *Appl Sci* 10:9020. <https://doi.org/10.3390/app10249020>
- Xu H (2006) Modification of normalised difference water index (NDWI) to enhance open water features in remotely sensed imagery. *Int J Remote Sens* 27:3025–3033. <https://doi.org/10.1080/01431160600589179>
- Xu H (2010) Analysis of impervious surface and its impact on urban heat environment using the normalized difference impervious surface index (NDISI). *Photogramm Eng Remote Sens* 76:557–565. <https://doi.org/10.14358/PERS.76.5.557>
- Xu X, Sun S, Liu W et al (2017) The cooling and energy saving effect of landscape design parameters of urban park in summer: a case of Beijing, China. *Energy Build* 149:91–100. <https://doi.org/10.1016/j.enbuild.2017.05.052>
- Yan H, Wu F, Dong L (2018) Influence of a large urban park on the local urban thermal environment. *Sci Total Environ* 622–623:882–891. <https://doi.org/10.1016/j.scitotenv.2017.11.327>
- Yue W, Qiu S, Xu H et al (2019) Polycentric urban development and urban thermal environment: a case of Hangzhou, China. *Landsc Urban Plan* 189:58–70. <https://doi.org/10.1016/j.landurbplan.2019.04.008>
- Zak M, Nita I-A, Dumitrescu A, Cheval S (2020) Influence of synoptic scale atmospheric circulation on the development of urban heat island in Prague and Bucharest. *Urban Clim* 34:100681. <https://doi.org/10.1016/j.uclim.2020.100681>

Publisher's note Springer Nature remains neutral with regard to jurisdictional claims in published maps and institutional affiliations.

Springer Nature or its licensor (e.g. a society or other partner) holds exclusive rights to this article under a publishing agreement with the author(s) or other rightsholder(s); author self-archiving of the accepted manuscript version of this article is solely governed by the terms of such publishing agreement and applicable law.